12-2012

Investigation of Shroud Geometry to Passively Improve Heat Transfer in a Solar Thermal Storage Tank

Matthew Keene Zemler
Embry-Riddle Aeronautical University - Daytona Beach

INVESTIGATION OF SHROUD GEOMETRY TO PASSIVELY IMPROVE HEAT TRANSFER IN A SOLAR THERMAL STORAGE TANK

by

Matthew Keene Zemler

A Thesis Submitted to the College of Engineering Department of Mechanical Engineering in Partial Fulfillment of the Requirements for the Degree of Master of Science in Mechanical Engineering

Embry-Riddle Aeronautical University
Daytona Beach, Florida
December 2012

INVESTIGATION OF SHROUD GEOMETRY TO PASSIVELY IMPROVE HEAT TRANSFER IN A SOLAR THERMAL STORAGE TANK

by

Matthew Keene Zemler

This thesis was prepared under the direction of the candidate's Thesis Committee Chair, Dr. Sandra K. S. Boetcher, Professor, Daytona Beach Campus, and Thesis Committee Members Dr. Birce Dikici, Professor, Daytona Beach Campus, and Mr. Rafael Rodriguez, Professor, Daytona Beach Campus, and has been approved by the Thesis Committee. It was submitted to the Department of Mechanical Engineering in partial fulfillment of the requirements for the degree of Master of Science in Mechanical Engineering

Thesis Review Committee:

Sandra K. S. Boetcher, Ph.D.
Committee Chair

Birce Dikici, Ph.D.
Committee Member

Rafael Rodriguez, MSME P.E.
Committee Member

Darris L. White, Ph.D.
Graduate Program Chair,
Mechanical Engineering

Charles F. Reinholtz, Ph.D.
Department Chair,
Mechanical Engineering

Maj Mirmirani, Ph.D.
Dean, College of Engineering

Robert Oxley, Ph.D.
Associate Vice President of Academics

12/14/12
Date

Acknowledgements

I would like to express my deepest appreciation and gratitude to my advisor, Dr. Sandra K. S. Boetcher, for the patient guidance and encouragement she provided to me throughout my undergraduate studies at The University of North Texas all the way through the completion of this degree at Embry-Riddle Aeronautical University. Dr. Sandra K. S. Boetcher has been more than just a professor to me for the last few years; she has been a mentor, colleague, and friend and I am truly fortunate to have had the opportunity to know her.

I owe a great deal of gratitude to the individuals in the Mechanical Engineering Department, especially Dr. Charles Reinholtz, who gave me the opportunity to enrich my engineering understanding at this university.

I am grateful for my friends' and families' endless encouragement and support throughout my master's education. My wife, Kelsey, has been my inspiration and rock through the good and bad times. Without all the support and encouragement given to me, I would not have been able to maintain the motivation to complete this degree.

Abstract

Researcher: Matthew Keene Zemler

Title: Investigation of Shroud Geometry to Passively Improve Heat Transfer in a Solar Thermal Storage Tank

Institution: Embry-Riddle Aeronautical University

Degree: Master of Science in Mechanical Engineering

Year: 2012

A shroud and baffle configuration is used to passively increase heat transfer in a thermal store. The shroud and baffle are used to create a vena contracta near the surface of the heat exchanger, which will speed up the flow locally and thereby increasing heat transfer. The goal of this study is to investigate the geometry of the shroud in optimizing heat transfer by locally increasing the velocity near the surface of the heat exchanger. Two-dimensional transient simulations are conducted. The immersed heat exchanger is modeled as an isothermal cylinder, which is situated at the top of a solar thermal storage tank containing water (Pr = 3) with adiabatic walls. The shroud and baffle are modeled as adiabatic, and the geometry of the shroud and baffle are parametrically varied. Nusselt numbers and fractional energy discharge rates are obtained for a range of Rayleigh numbers, $10^5 \leq Ra_D \leq 10^7$, in order to determine optimal shroud and baffle configurations.

Table of Contents

Page

List of Figures

Chapter I

Introduction

A solar thermal storage tank is a key component used in domestic solar hot water systems. The thermal energy can be transferred from a solar thermal storage tank either directly or indirectly. The design of a direct thermal store requires the hot or cold fluid to directly flow into the tank where as an indirect design would use a heat exchanger to transfer the thermal energy.

Since the design of a direct thermal store requires the fluid to flow directly into the tank, the storage fluid is required to be compatible with potable water. This is an advantage of using an indirect over a direct design since the store fluid can be selected for its thermal properties rather than its compatibility with potable water.

Statement of Problem

Solar thermal storage tanks typically are configured to take advantage of stratification to exchange heat by way of natural convection. In the charging process (the heat is transferred from the heat exchanger to the tank), the immersed heat exchanger is situated near the bottom of the storage tank. Likewise, in the discharging process (the heat is transferred from the tank to the heat exchanger), the immersed heat exchanger is situated near the top of the storage tank (Fig. 1.1). The current study focuses on passively increasing the heat transfer rate by more effectively controlling the flow around the immersed heat exchanger, using a shroud and baffle in a storage tank during the discharge process.

Background

There are two established modes of passively increasing heat transfer. The first is to maintain a large temperature difference between the heat exchanger and the ambient fluid for as long as possible, and the second is to increase the outer velocity of the fluid in the vicinity of the heat exchanger. A technique to maintain a large temperature difference between the heat exchanger and the ambient fluid is to make sure that the buoyant plume from the heat exchanger travels the entire length of the tank and does not "short-circuit." This can be accomplished through the use of long baffles, which direct the flow from the plume to go all the way to the bottom of the tank. Furthermore, a shroud can be used to create a vena contracta near the surface of the heat exchanger, which will speed up the flow locally and thereby increasing heat transfer.

Controlling the fluid motion in the tank is critical for optimizing heat transfer, which increases discharging rates [1]. Researchers over the years have experimented with different methods of passively achieving maximum heat transfer. Early on, investigators focused on trying to maintain stratification in the tank by experimenting with a baffle located under a coiled heat exchanger [2 – 4]. Chauvet *et al.* [5] found that by placing a baffle beneath the heat exchanger, the velocity of the flow near the heat exchanger increases.

Su and Davidson [6] demonstrated that a straight, cylindrical baffle (compared to no baffle and a more complex baffle that impedes the flow) placed underneath an immersed heat exchanger was the most beneficial in increasing the heat transfer, and Haltiwanger and Davidson [7] experimentally verified the increase in heat transfer due to a straight baffle.

Although much numerical and experimental work exists regarding increasing heat transfer by passive means, very little work has been performed to optimize shroud and baffle geometries. Kulacki *et al.* [8] performed analytical work on a straight baffle placed underneath a heat exchanger modeled as a two-dimensional cylinder. Follow-on work by Boetcher *et al.* [9] focused on using baffles of different lengths to slow flow and reduce mixing in the tank. Another study by Boetcher *et al*. [10] focused on using a shroud of varying sizes to increase the velocity of the flow near the heat exchanger. It was found that using a shroud increased the heat transfer and thermal storage tanks discharged faster.

The work presented here is a continuation of the parametric studies found in [9] and [10] that examine the discharge case. These studies examined the effects of varying the length of the baffle, the distance W from the cylinder, and the amount of the shroud on the heat transfer rate of the solar thermal storage tank. The heat exchanger is modeled as a two-dimensional isothermal cylinder situated at the top of a thermal storage tank. The simplistic model of the heat exchanger-tank geometry is for gaining insight into the optimal passive mechanisms for increasing heat transfer. The optimal shroud height and baffle length are used from the previous studies, and the baffle and shroud widths are varied. Numerical simulations are performed for $10^5 < Ra_D < 10^7$ and Pr = 3 (water in the tank). Nusselt numbers and fractional energy discharges are also presented.

Nomenclature

a	shroud angle
c_p	specific heat at constant pressure
D	diameter of the cylinder

f	fractional energy discharge
g	gravitational constant
Gr_D	Grashof number, $g\beta\,(T_{initial} - T_{cylinder})D^3/\nu^2$
H	height of shroud
h	average heat transfer coefficient
k	thermal conductivity of the fluid
L	length of baffle
L_c	characteristic length
Nu_D	average Nusselt number
P	dimensionless pressure, $p - p_\infty/\rho(\nu/D)^2$
p	pressure
p_∞	free-stream pressure
Pr	Prandtl number, $c_p\mu/k$
R	radius of curvature of shroud
Ra_D	Rayleigh number, Gr_DPr
T	temperature
T_{ave}	average temperature of the fluid in the tank
$T_{cylinder}$	temperature at surface of cylinder
$T_{initial}$	initial temperature of fluid in tank
t	time
t_B	baffle thickness
U, V	dimensionless velocity components, $(u, v)/(\nu/D)$
u, v	velocity components

W	width of baffle
X, Y	dimensionless Cartesian coordinates, (x, y)/D
x, y	Cartesian coordinates
Greek	
β	isobaric coefficient of thermal expansion
θ	dimensionless temperature, $(T - T_{cylinder})/(T_{initial} - T_{cylinder})$
ν	kinematic viscosity of the fluid
ρ	density of the fluid
τ	dimensionless time, $t\nu/D^2$
μ	dynamic viscosity

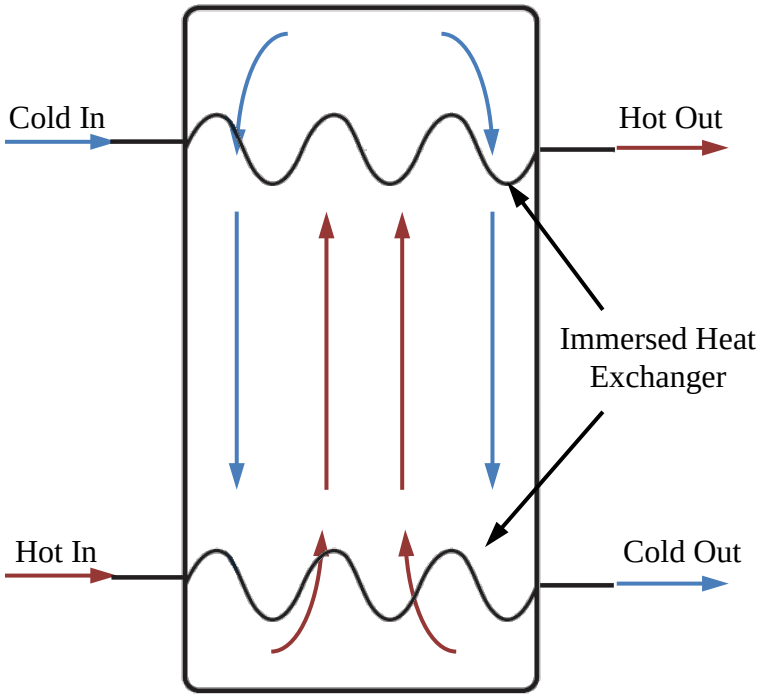

Figure 1.1. Schematic diagram of the immersed heat exchangers in a thermal store.

Chapter II

Problem Formulation

In order to model an insulated solar thermal storage tank, several steps are performed to analyze the desired results, which consist of constructing the solution domain, mesh, the physic-definition preprocess, and the post processing.

Physical Model and Solution Domain

The heat exchanger is modeled as a two-dimensional cylinder situated in an insulated solar thermal storage tank. Since the tank is geometrically and thermally symmetric, only half of the tank is modeled. The dimensions of the tank and baffle-shroud assembly are shown in Fig. 2.1 and a three-dimensional rendering of the tank and a detailed drawing of the cylinder and the shroud-baffle is conveyed in Fig. 2.2. The dimensionless quantities are based on a cylinder diameter D = 2.86 cm and a tank which is 121.9 cm tall and 10.2 cm wide [11]. In the figures, D is the diameter of the cylinder, L = 30D is the length of the baffle, H = 1.5D is the height of the shroud, R is the radius of curvature of the shroud, which is set equal to D, t_B = 0.111D is the thickness of the shroud/baffle, and W is the width of the baffle. The width of the baffle is parametrically varied $0.25D \leq W \leq 1.25D$.

Governing Equations

The following dimensionless variables are used in writing the governing equations

$$(\mathbf{U},\mathbf{V}) = \frac{(\mathbf{u},\mathbf{v})}{\frac{\boldsymbol{\upsilon}}{\mathbf{D}}}, \quad (\mathbf{X},\mathbf{Y}) = \frac{(\mathbf{x},\mathbf{y})}{\mathbf{D}}, \quad \mathbf{P} = \frac{\mathbf{p} - \mathbf{p}_\infty}{\boldsymbol{\rho}\left(\frac{\boldsymbol{\upsilon}}{\mathbf{D}}\right)^2}$$

$$\boldsymbol{\theta = \frac{T - T_{cylinder}}{T_{initial} - T_{cylinder}}, \quad \tau = \frac{t\nu}{D^2}} \tag{2.1}$$

Here, u and v are the velocity components in the x- and y- directions respectively. D is the outside diameter of the cylinder, p is the pressure, T is the temperature, $T_{cylinder}$ is the surface temperature of the cylinder, $T_{initial}$ is the buoyancy reference temperature, which is the initial temperature of the fluid in the tank, ρ is the fluid density, ν is the kinematic viscosity of the fluid, and t is the time. Since ν/D has units of velocity, it will be used as the velocity reference quantity.

Additionally, the Grashof number based on the diameter of the cylinder Gr_D, the Prandtl number Pr, and the Rayleigh number Ra_D are used in the dimensionless equations.

$$\boldsymbol{Gr_D = \frac{g\beta(T_{initial} - T_{cylinder})D^3}{\nu^2}, \quad Pr = \frac{c_p\mu}{k}, \quad Ra_D = Gr_D Pr} \tag{2.2}$$

In these dimensionless groups, g is the acceleration of gravity, β is the coefficient of thermal expansion for the fluid, c_p is the specific heat at constant pressure, μ is the dynamic viscosity, and k is the thermal conductivity of the fluid.

The dimensionless form of the equations for laminar transient incompressible natural convection flow are

Conservation of Mass

$$\boldsymbol{\frac{\partial U}{\partial X} + \frac{\partial V}{\partial Y} = 0} \tag{2.3}$$

Conservation of Momentum in the X-Direction

$$\frac{\partial U}{\partial \tau}+\frac{\partial U^2}{\partial X}+\frac{\partial (UV)}{\partial Y}=-\frac{\partial P}{\partial X}+\frac{\partial^2 U}{\partial X^2}+\frac{\partial^2 U}{\partial Y^2}+Gr_D(\theta-1) \tag{2.4}$$

Conservation of Momentum in the Y-Direction

$$\frac{\partial V}{\partial \tau}+\frac{\partial (UV)}{\partial X}+\frac{\partial V^2}{\partial Y}=-\frac{\partial P}{\partial Y}+\frac{\partial^2 V}{\partial X^2}+\frac{\partial^2 V}{\partial Y^2} \tag{2.5}$$

Conservation of Energy

$$\frac{\partial \theta}{\partial \tau}+\frac{\partial (UV)}{\partial X}+\frac{\partial (V\theta)}{\partial Y}=\frac{1}{Pr}\left[\frac{\partial^2 \theta}{\partial X^2}+\frac{\partial^2 \theta}{\partial Y^2}\right] \tag{2.6}$$

In the X-direction momentum equation, the Boussinesq approximation is employed because of the small temperature differences encountered in natural convection. In the energy equation, viscous dissipation and compression work terms are neglected due to the small velocities.

Boundary and Initial Conditions

At the surface of the cylinder, the dimensionless boundary conditions are

$$U=V=0 \text{ and } \theta=0 \tag{2.7}$$

The walls of the storage tank and the cylinder and shroud assembly are adiabatic

$$U=V=0 \text{ and } \frac{\partial \theta}{\partial n}=0 \tag{2.8}$$

where n is the surface normal. The dimensionless boundary conditions at the line of symmetry are

$$\frac{\partial U}{\partial y} = \frac{\partial \theta}{\partial y} = 0 \text{ and } V = 0 \tag{2.9}$$

The dimensionless initial conditions of the storage tank are

$$U = V = 0, \quad \theta = 1, \quad \text{and } P = 0 \text{ at } \tau = 0 \tag{2.10}$$

Pre-Processing

The solution domain and mesh were created in Pro-Engineer Wildfire 5.0 and ANSYS CFX 13.0, respectively. Due to the solar thermal storage tank's geometric and thermal symmetry, a two-dimensional cylinder situated in an insulated solar thermal storage tank was constructed to minimize both computational resources and time.

An automatic patch conforming tetrahedral mesh was created in ANSYS Workbench 13.0, seen in Figure 2.3. Tetrahedral and hexahedral elements were used in combination while constructing the mesh, which allowed for fluid and thermal boundary layers to be resolved. To resolve the boundary layer at the cylinder and shroud, an inflation boundary profile was created to concentrate more elements near the desired boundaries.

The maximum and minimum element size allowed for the constructed mesh is 0.035 meters and 0.005 meters, respectively. This resulted in the mesh using 120,000 nodes, which created 57,000 elements.

In order to define the boundary conditions, fluid properties, and fluid characteristics, the patch conforming tetrahedral mesh was imported into ANSYS CFX-Pre, which is the physics-definition pre-processor for ANSYS CFX. Once the boundary conditions, fluid properties, and fluid characteristics are applied, a definition file is created. This definition file contains all the necessary information to run the simulation.

The simulations are organized based on shroud distance and Rayleigh numbers. A natural convection problem uses the Rayleigh number to determine if the flow is laminar, $Ra_D < 10^9$, or turbulent, $Ra_D > 10^9$. The dimensionless Rayleigh number is the product of two other dimensionless numbers, which are the Grashof and Prandtl numbers. The Grashof number describes the relationship between the buoyant and viscous forces of a given fluid, and the Prandtl number describes the relationship between the momentum diffusivity and the thermal diffusivity.

Solution

The numerical simulations were performed using commercial software, ANSYS CFX 13.0, which employs a coupled multi-grid solver. A mesh-independence study was conducted for $Ra_D = 10^7$, which was chosen because the thinnest boundary layers are found at this Rayleigh number. The test case chosen was W = 0.75D. The number of nodes was increased from 120,000 to approximately 200,000, and the solution was run until τ was approximately 0.02. The Nusselt numbers varied by less than 5%; therefore, the number of nodes used was 120,000. The time-step required is very small since natural convection is inherently unstable. The timestep used here was $\Delta\tau = 0.0001$.

A further check on the validity of the solutions was to compare the Nusselt numbers obtained in the quasi-steady state (when the heat transfer results are almost equivalent to that of a cylinder in an infinite environment) with those of the well-known correlations of Morgan [12] and Churchill and Chu [13].

Post Processing

ANSYS CFX-Post was used to analyze the result files from the simulations. In order to calculate the average Nusselt number along the cylinder and average temperature of the thermal storage tank, ANSYS CFX-Post function calculator was utilized.

The Nusselt number is viewed as the dimensionless convection heat transfer coefficient.

$$\mathbf{Nu} = \frac{\mathbf{hL_c}}{\mathbf{k}} \tag{2.11}$$

In this dimensionless group, h is the convective heat transfer coefficient, k is the thermal conductivity of the fluid, and L_c is the characteristic length. The Nusselt number is the ratio of the convection and conduction heat fluxes. This ratio represents the increase of heat transfer across a fluid layer as a result of convection relative to conduction.

In order to calculate the average Nusselt number, the wall heat flux was extracted from the surfaces of the cylinder, which were in turn used to calculate the average convective heat transfer coefficient. The approach that ANSYS CFX-Post software uses to calculate the wall heat flux is by implementing the finite difference method, which would expand the function in terms of a Fourier series. This allows Fourier's law of heat conduction to be applied and extract the desired wall heat flux along the surface of the cylinder.

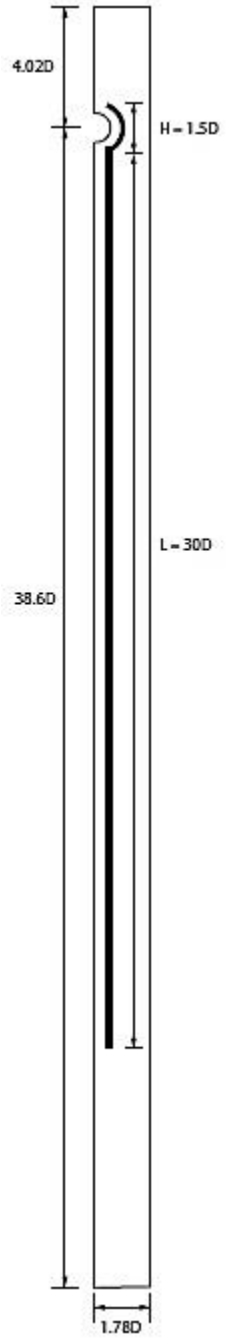

Figure 2.1. Solution domain for an isothermal cylinder with a shroud and baffle situated in a storage tank.

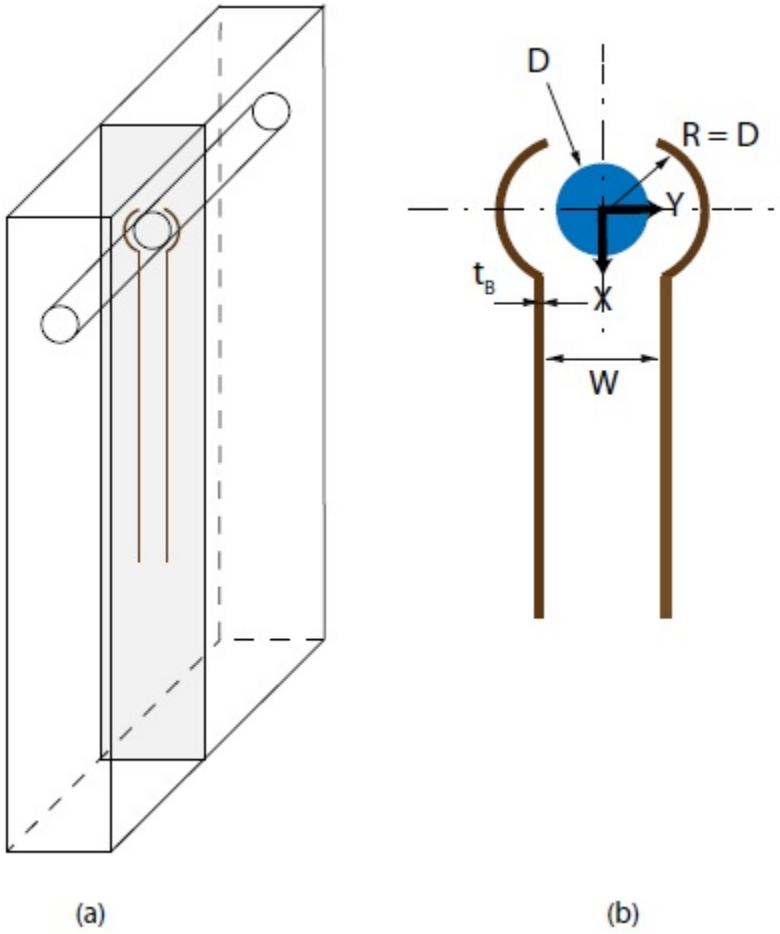

Figure 2.2. Schematic diagram of (a) the three-dimensional situation, and (b) the dimensions for the isothermal cylinder and adjacent shroud-baffle situated in a thermal storage tank.

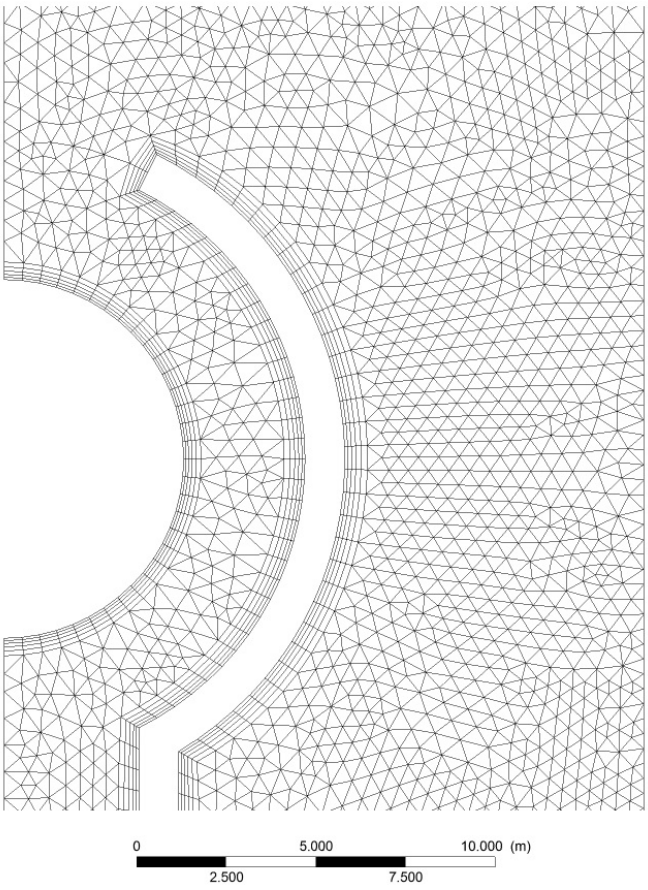

Figure 2.3. Solution mesh for an isothermal cylinder with a shroud and baffle situated in a storage tank.

Chapter III

Results

There are four transient heat transfer stages that occur in the discharge of thermal stores; conduction (very little fluid motion), quasi-steady (heat exchanger heat transfer behaves as if it is in an infinite environment), fluctuating (heat exchanger feels effect of enclosure), and decay [1, 14].

Shroud Distance

Average Nusselt numbers for the heat exchangers are graphed against dimensionless time in Figs. 3.1 – 3.3 for Rayleigh numbers, 10^5, 10^6, and 10^7, respectively. Plotted in the graphs for each Rayleigh number is a comparison of various shroud/baffle widths. Also shown in the graphs is the case where there is no baffle or shroud (none). Furthermore, all heat transfer transient regions are approximated by inspection of the figures.

As expected, during the conduction phase ($\tau \leq 0.01$ for $Ra_D = 10^5$, $\tau \leq 0.005$ for $Ra_D = 10^6$, and $\tau \leq 0.002$ for $Ra_D = 10^7$) where there is very little fluid motion, the shroud/baffle configuration has no effect on heat transfer. Next, moving into the quasi-steady phase ($0.01 \leq \tau \leq 0.1$ for $Ra_D = 10^5$, $0.005 \leq \tau \leq 0.04$ for $Ra_D = 10^6$, and $0.002 \leq \tau \leq 0.01$ for $Ra_D = 10^7$), the shroud/baffle has more of an effect on the heat transfer with greater the Rayleigh number.

The fluctuating period ($0.1 \leq \tau \leq 4$ for $Ra_D = 10^5$, $0.04 \leq \tau \leq 2$ for $Ra_D = 10^6$, and $0.01 \leq \tau \leq 1$ for $Ra_D = 10^7$) is when the presence of the shroud/baffle is most effective. As can be seen from the figures, certain shroud/baffle geometric configurations are more advantageous than others. It is during this period that the baffle width W = 0.75D

appears to be the optimal width for all three of the Rayleigh numbers. Interestingly, the baffle width W = 0.25D appears to be performing worse in some areas for $Ra_D = 10^5$ and 10^6 than if there were no shroud/baffle at all. Perhaps this tight of a restriction near the heat exchanger is choking the flow. To further investigate this, Fig. 3.4 has been prepared. In the figure, a comparison of velocity vector fields (velocity is dimensionless) for several different shroud/baffle widths is shown. This illustration shows that by keeping the shroud/baffle geometry the same and parametrically varying the width, the opening at the top for the fluid to flow by the heat exchanger becomes increasingly smaller.

Finally, the long decay period is when the Nusselt numbers asymptotically approach 0. The figures show that the more effective the shroud/baffle is in increasing heat transfer, the faster the Nusselt number will approach 0.

Another method of determining which shroud/baffle is most advantageous is to look at the fraction energy discharge [7], which is defined as

$$\mathbf{f} = \frac{\mathbf{T_{initial} - T_{ave}}}{\mathbf{T_{initial} - T_{cylinder}}} \tag{3.1}$$

In this equation, T_{ave} is the average temperature of the fluid in the thermal storage tank. The fractional energy discharge is a way of quantifying the amount of energy, which has been given up by the tank to the fluid in the heat exchanger. Figures 3.5 – 3.7 for Rayleigh numbers, 10^5, 10^6, 10^7, respectively, have been prepared to show the fractional energy discharge as a function of time.

The figures confirm that W = 0.75D is discharging the tank at a faster rate for all three of the Rayleigh numbers considered. Furthermore, the graphs show that the worst

performing configuration for the lowest Rayleigh number is W = 0.25D and W = 1.25D for $Ra_D = 10^6$ and $Ra_D = 10^7$. Another trend is that the shroud/baffle configuration seems to make the most difference for the lowest Rayleigh number. This can be explained by the fact that the higher the Rayleigh number, the thinner the boundary layer. The faster moving fluid in the higher Rayleigh numbers is less affected by the vena contracta effect of the shroud/baffle.

The time it takes for the tank to discharge 70% of its initial energy will be used as the reference for comparison. Using the values for kinematic viscosity of water $\nu = 8.93 \times 10^{-7}$ and D = 2.86 cm, one unit of dimensionless time ($\tau = 1$) is approximately 15 minutes. By inspection of the graphs, for $Ra_D = 10^5$, the dimensionless time it takes for the tank to discharge the tank 70% for W = 0.25D (the worst case) and 0.75D (the best case) is 14.1 and 11.1, respectively. That equates to a real time difference of approximately 45 minutes.

Likewise, the time differences between the worst (W = 1.25D) and best (W = 0.75D) cases for $Ra_D = 10^6$ is approximately 15 minutes, and for $Ra_D = 10^7$, it is about 7.5 minutes.

Shroud Angle

Since the shroud and baffle perform poorly for W = 0.25D due to the small opening choking the flow (see Fig. 3.4), the shroud tilt angle a (Fig. 3.8) was parametrically varied between 0° and 5°. Figures 3.9 – 3.11 have been prepared for W = 0.25D and a = 0°, 2.5°, 5° to show the average Nusselt number versus dimensionless time. Also plotted on the graphs for reference is the optimal baffle width W = 0.75D with no shroud tilt (a = 0°). It is clear from the figures that tilting the shroud and

increasing the width of the opening at the top does not have a positive effect on heat transfer.

Figures 3.12 – 3.14 for W = 0.25D and a = 0°, 2.5°, 5° show the fractional energy discharge as a function of time. When these values are compared to the optimum baffle width, W = 0.75D with no shroud tilt (a = 0°), it can be seen that varying the tilt angle decrease the heat transfer rate. By using 70% fractional energy discharge as a reference comparison, for $Ra_D = 10^5$ and a = 2.5°, 5° the real time difference to the optimum baffle width is approximately 65 minutes and 71 minutes, respectively.

In trying to improve the heat transfer rate for W = 0.75D, the shroud tilt angle a was parametrically varied between 0° and 5°. Due to parametrically varying the shroud tilt angle, it negatively affected the heat transfer rate by decreasing the velocity at the cylinder. Figures 3.15 – 3.17 have been prepared for W = 0.75D and a = 0°, 2.5°, 5° to show the average Nusselt number versus dimensionless time. Not having a shroud/baffle configuration is also plotted on the graphs for reference.

For W = 0.75D and a = 0°, 2.5°, 5°, Figures 3.18 – 3.20 have been prepared to show the fractional energy discharge as a function of time. When comparing the shroud tilt angle to the optimum baffle width of W = 0.75D with no shroud tilt, it can be seen that increasing the angle decreases the heat transfer rate. This is due to decreasing the vena contracta effect on the baffle/shroud configuration. When comparing the angled results for $Ra_D = 10^5$ at a = 2.5° and 5° to the optimum baffle width, the real time difference is approximately 47 minutes and 50 minutes, respectively.

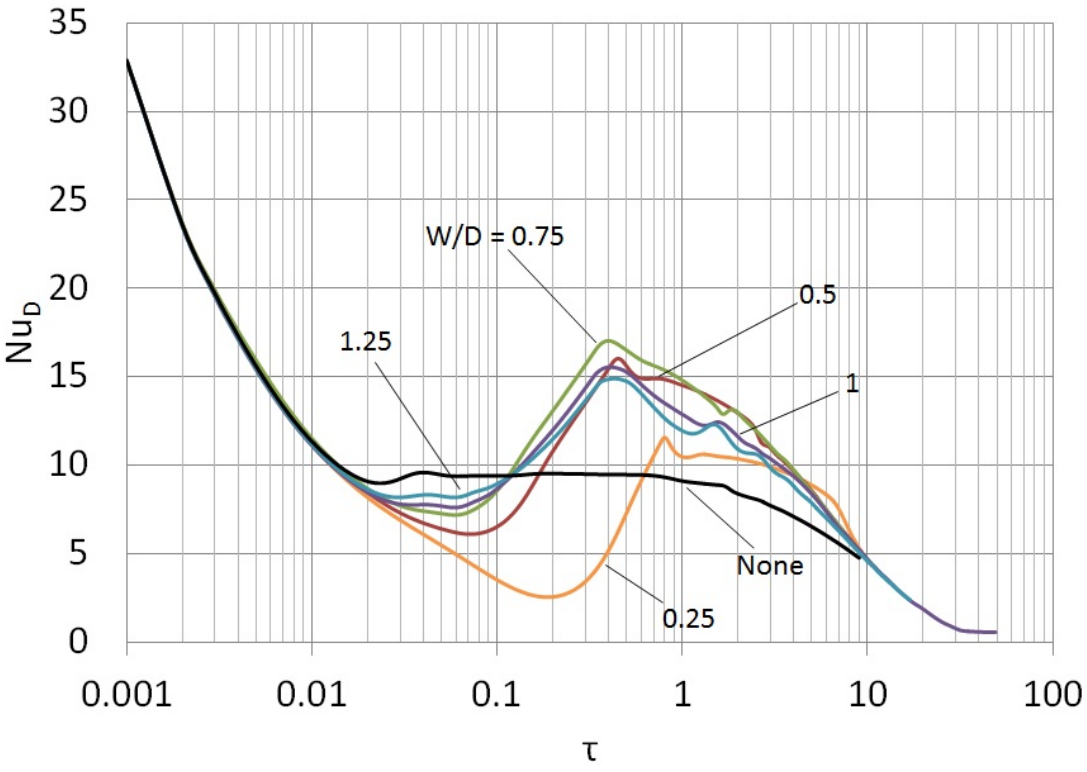

Figure 3.1. Average Nusselt number versus dimensionless time for $Ra_D = 10^5$.

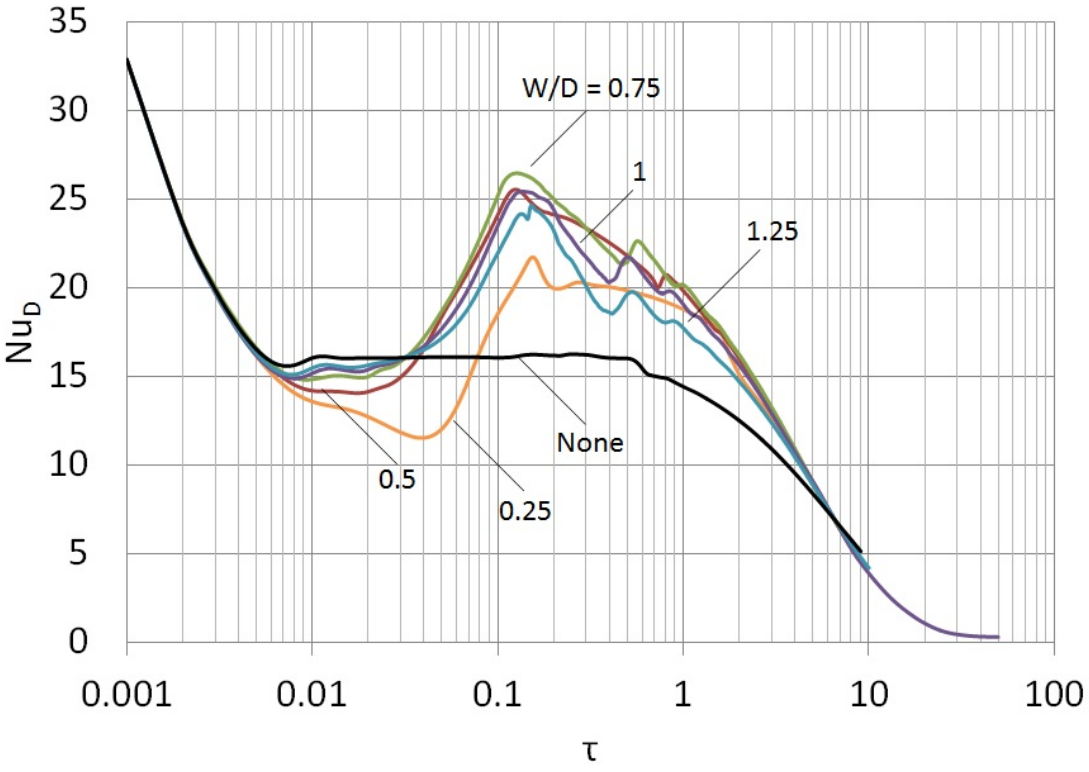

Figure 3.2. Average Nusselt number versus dimensionless time for $Ra_D = 10^6$.

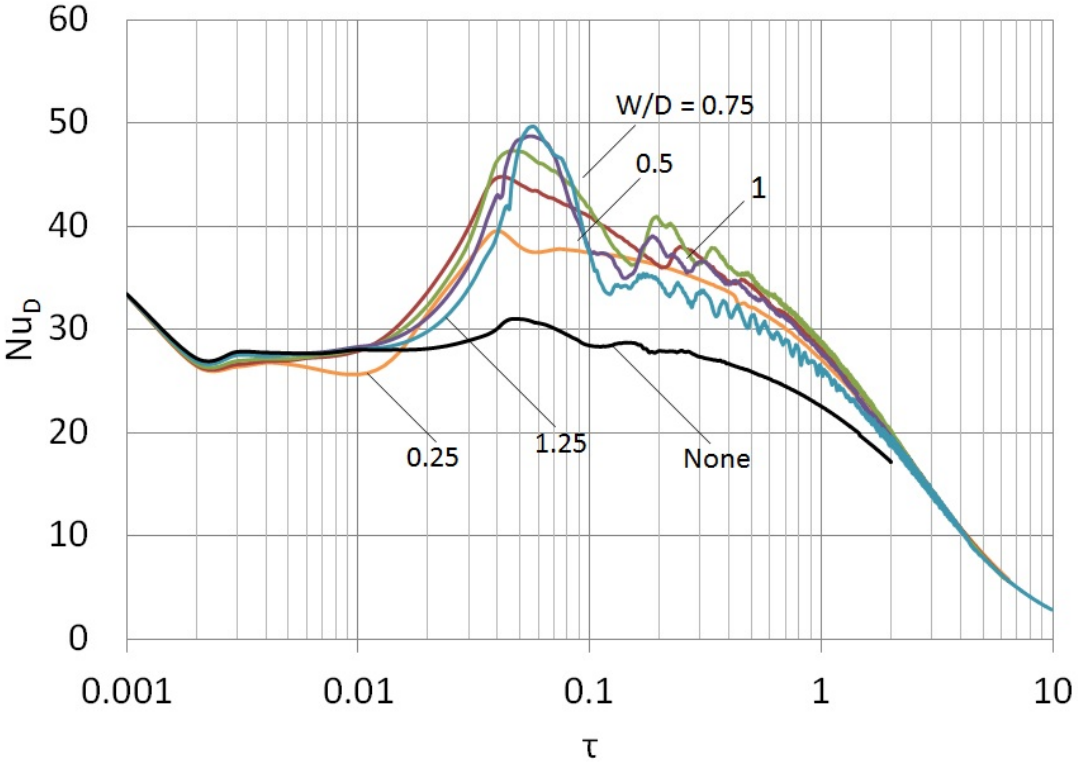

Figure 3.3. Average Nusselt number versus dimensionless time for $Ra_D = 10^7$.

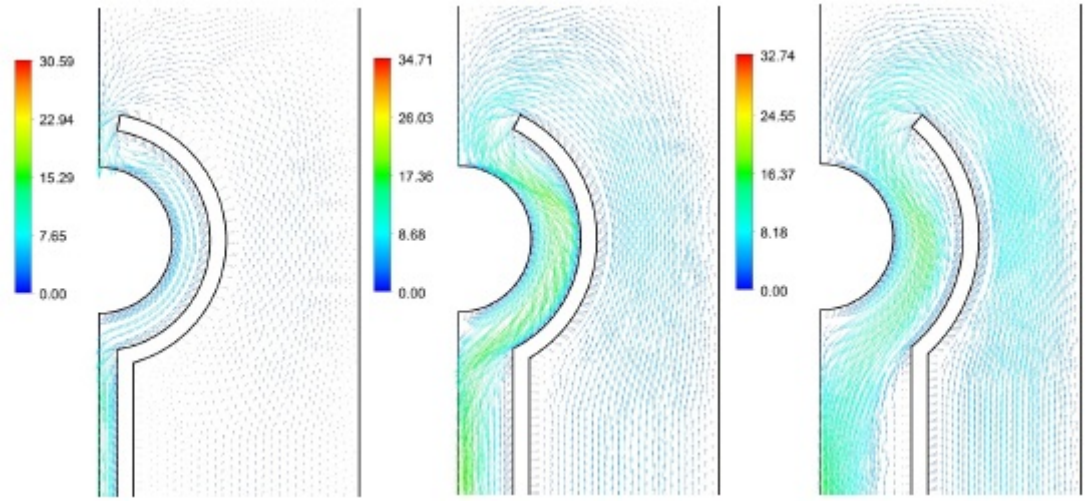

(a) (b) (c)

Figure 3.4. Velocity vector diagrams for $Ra_D = 10^5$ at $\tau = 2$ for (a) W = 0.25D, (b) W = 0.75D, (c) W = 1.25D

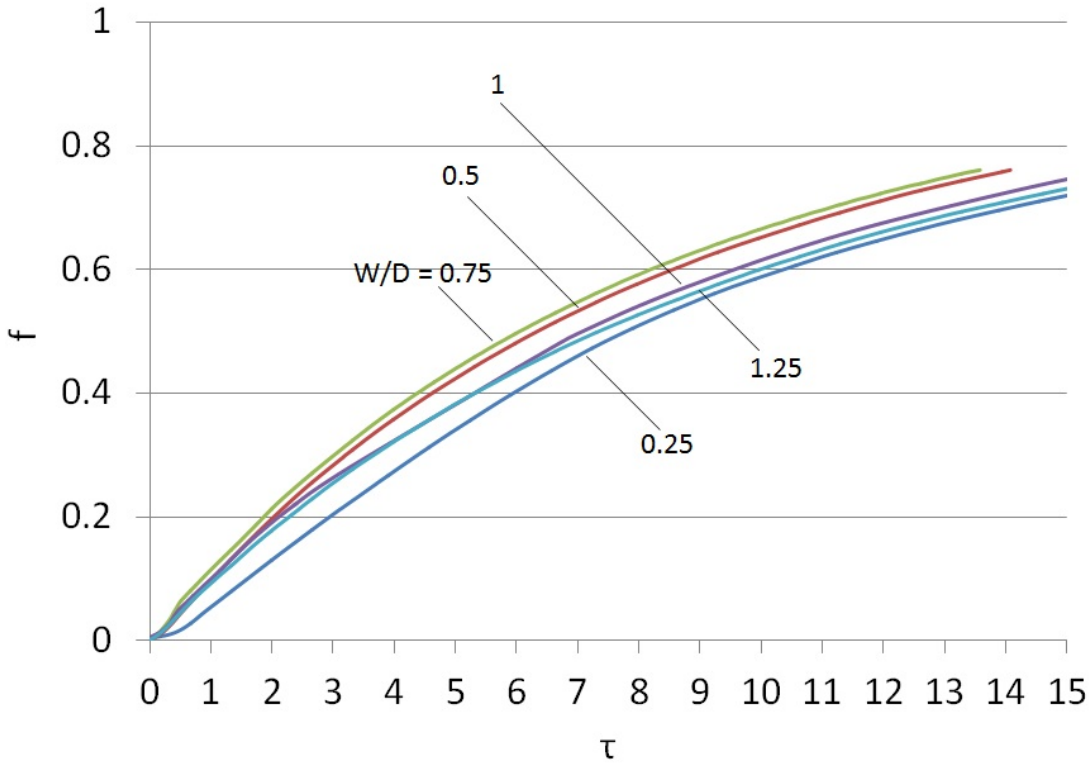

Figure 3.5. Fractional energy discharge versus dimensionless time for $Ra_D = 10^5$.

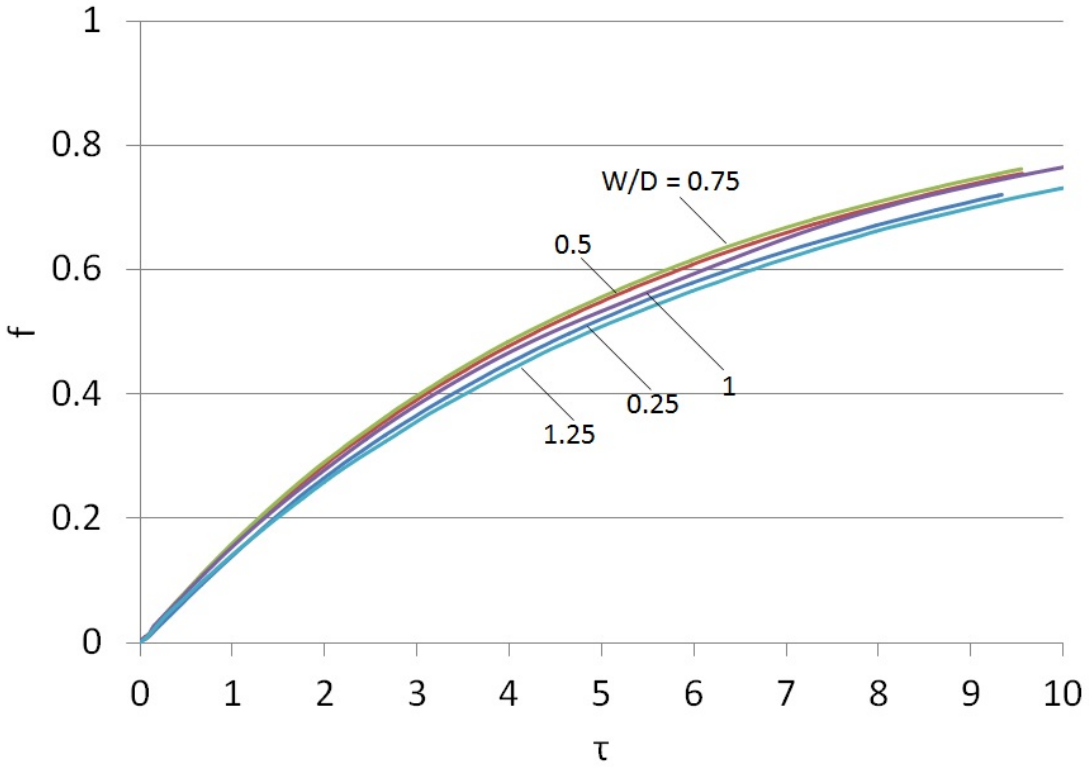

Figure 3.6. Fractional energy discharge versus dimensionless time for $Ra_D = 10^6$.

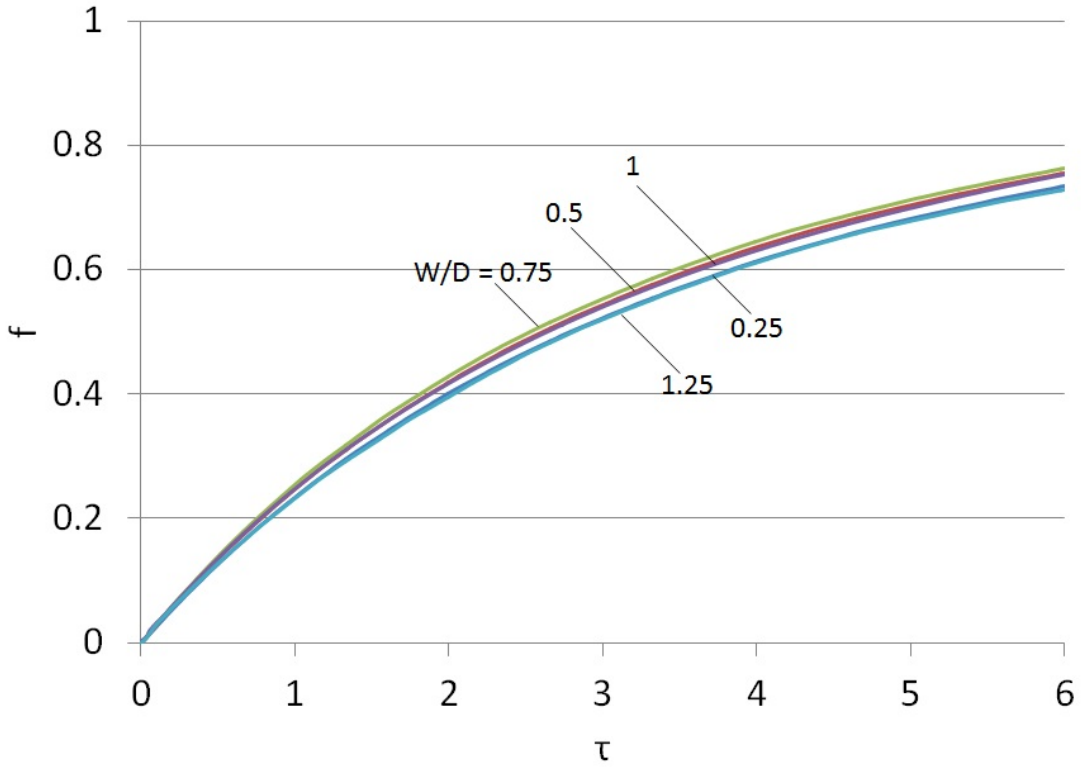

Figure 3.7. Fractional energy discharge versus dimensionless time for $Ra_D = 10^7$.

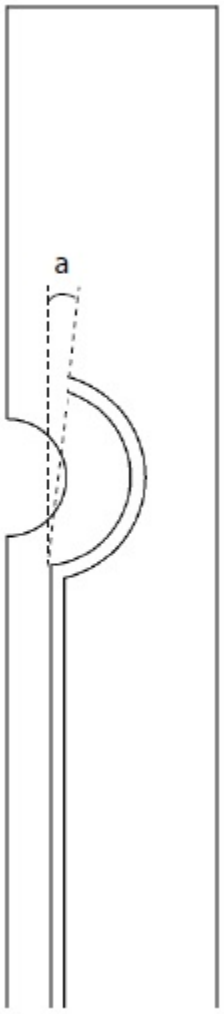

Figure 3.8. Schematic diagram showing the shroud angle.

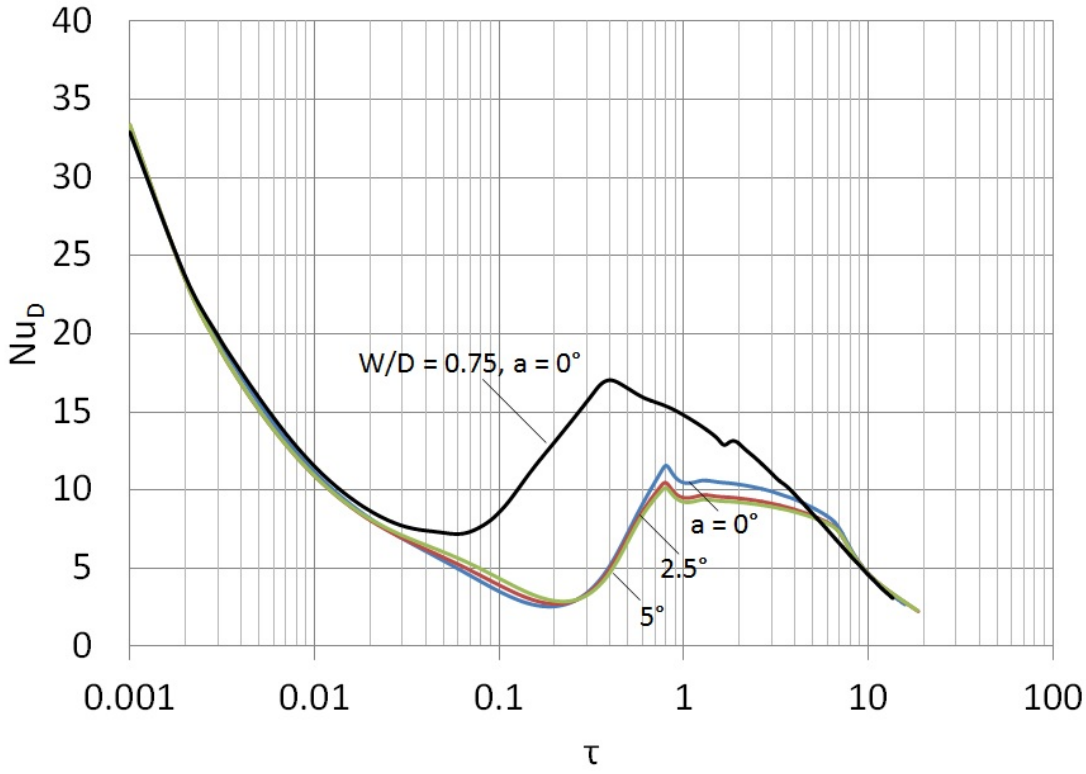

Figure 3.9. Average Nusselt number versus dimensionless time for $Ra_D = 10^5$, W/D = 0.25 and various shroud angles.

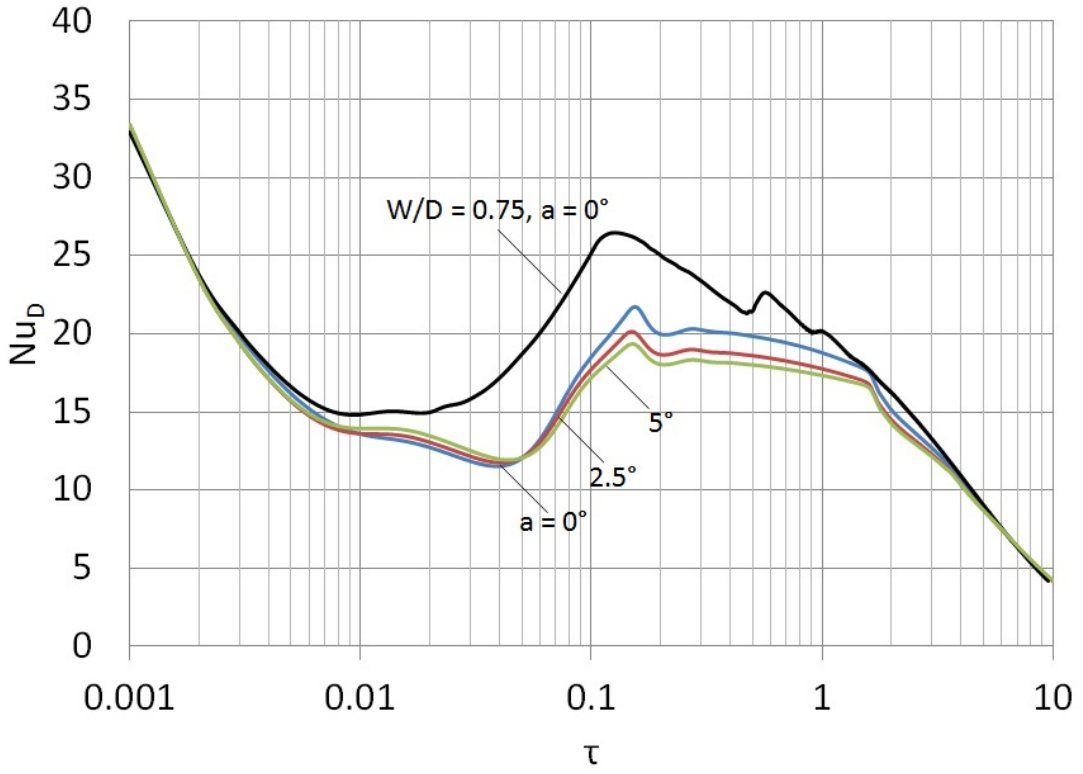

Figure 3.10. Average Nusselt number versus dimensionless time for $Ra_D = 10^6$, W/D = 0.25 and various shroud angles.

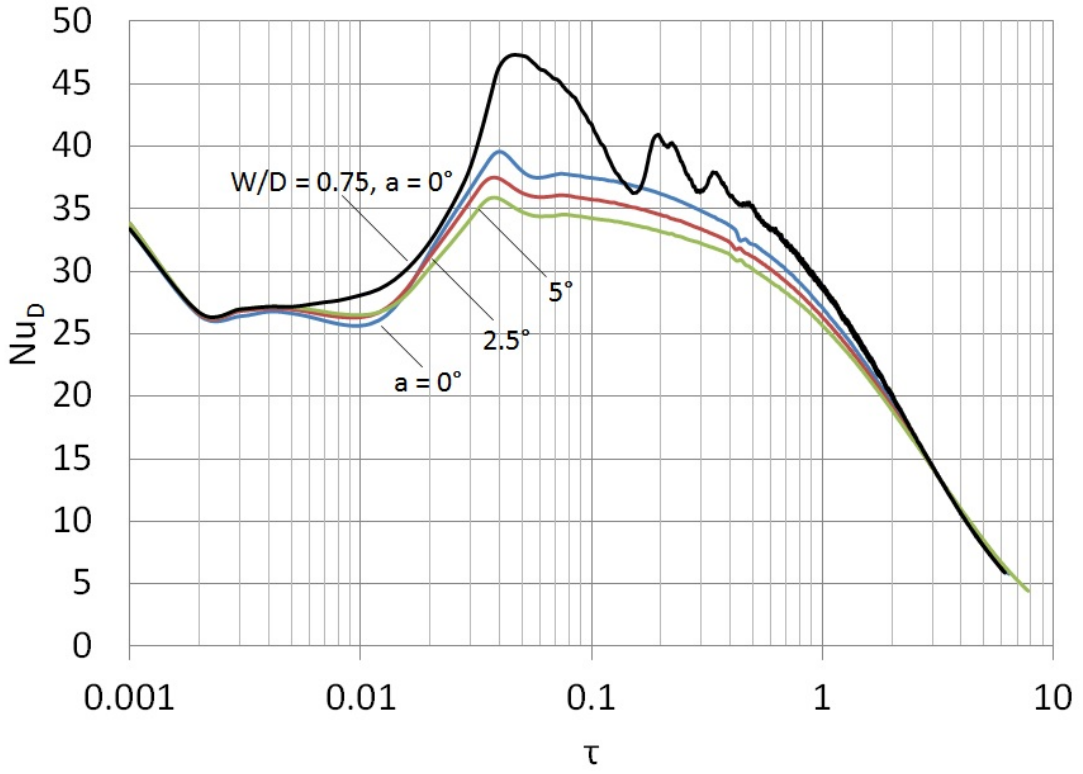

Figure 3.11. Average Nusselt number versus dimensionless time for $Ra_D = 10^7$, W/D = 0.25 and various shroud angles.

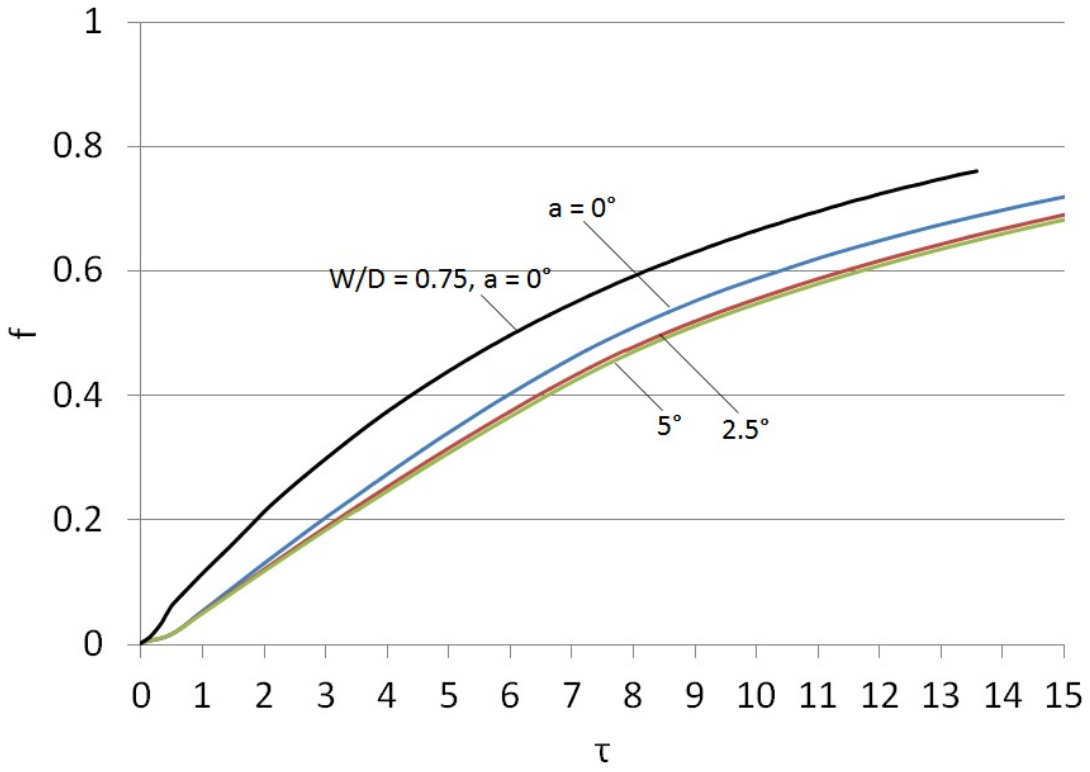

Figure 3.12. Fractional energy discharge versus dimensionless time for $Ra_D = 10^5$, W/D = 0.25 and various shroud angles.

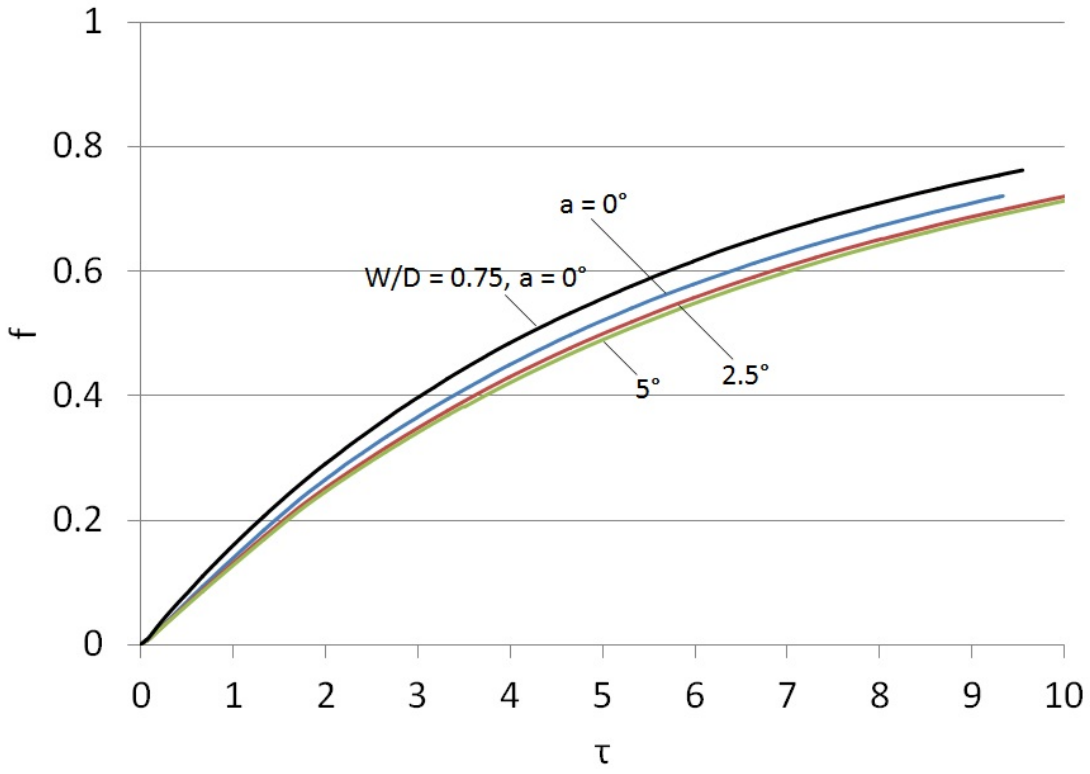

Figure 3.13. Fractional energy discharge versus dimensionless time for $Ra_D = 10^6$, W/D = 0.25 and various shroud angles.

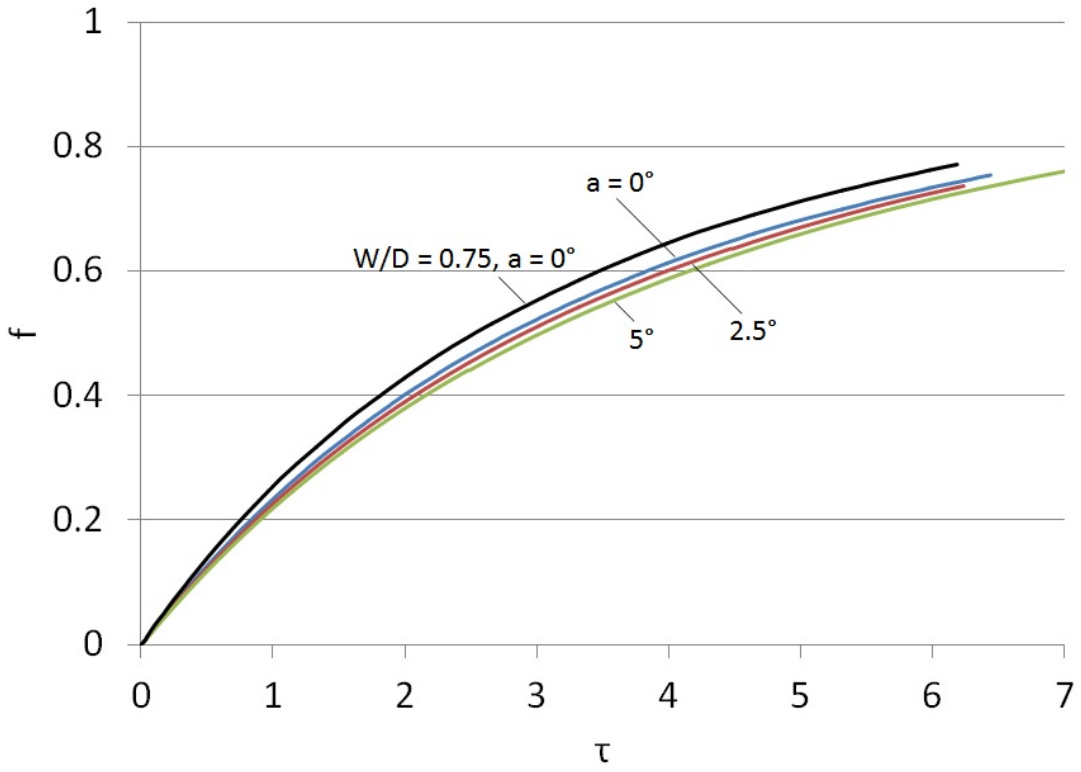

Figure 3.14. Fractional energy discharge versus dimensionless time for $Ra_D = 10^7$, W/D = 0.25 and various shroud angles.

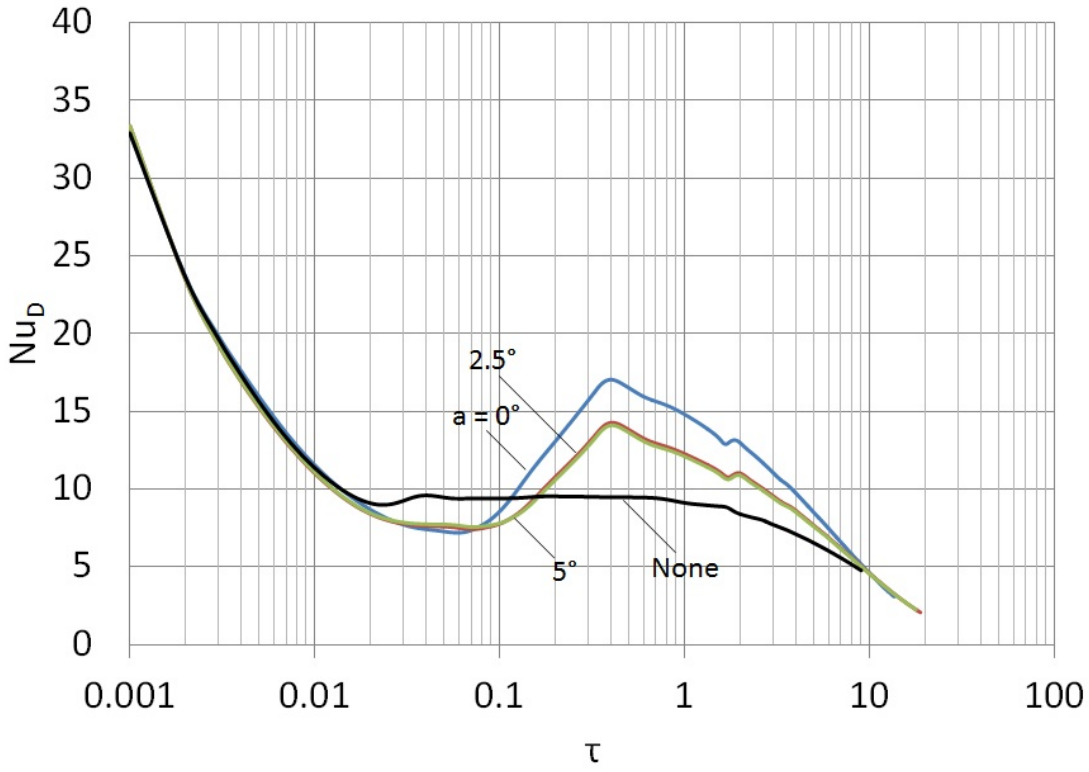

Figure 3.15. Average Nusselt number versus dimensionless time for $Ra_D = 10^5$, W/D = 0.75 and various shroud angles.

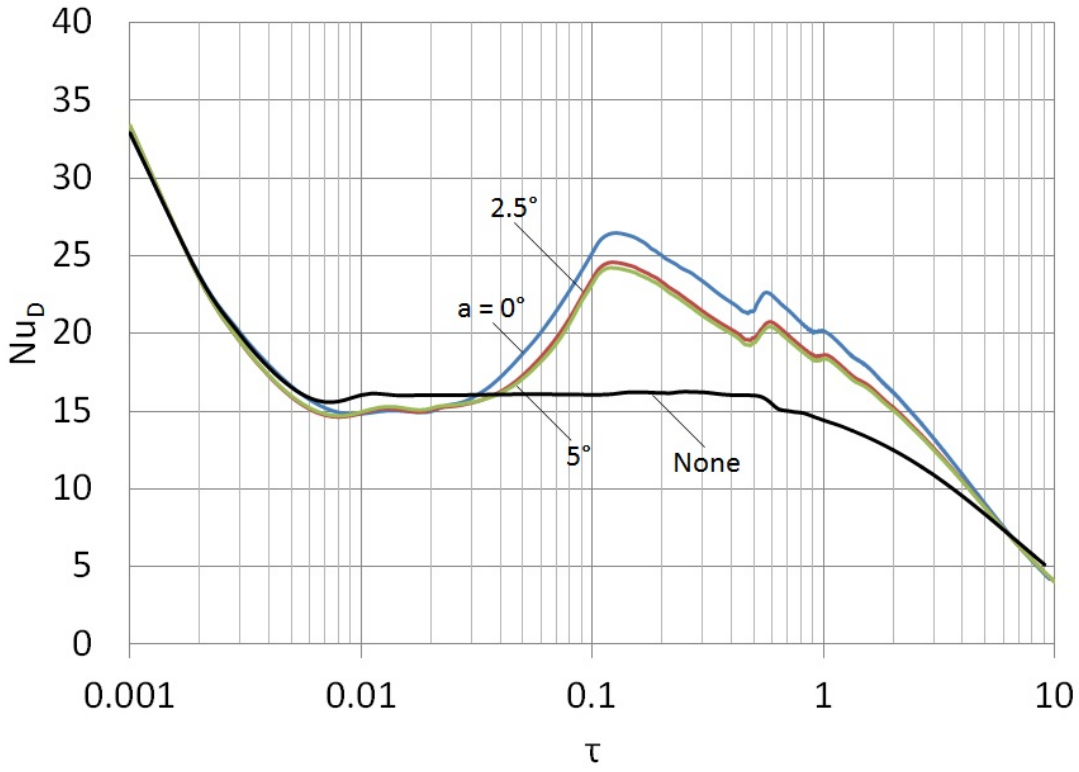

Figure 3.16. Average Nusselt number versus dimensionless time for $Ra_D = 10^6$, W/D = 0.75 and various shroud angles.

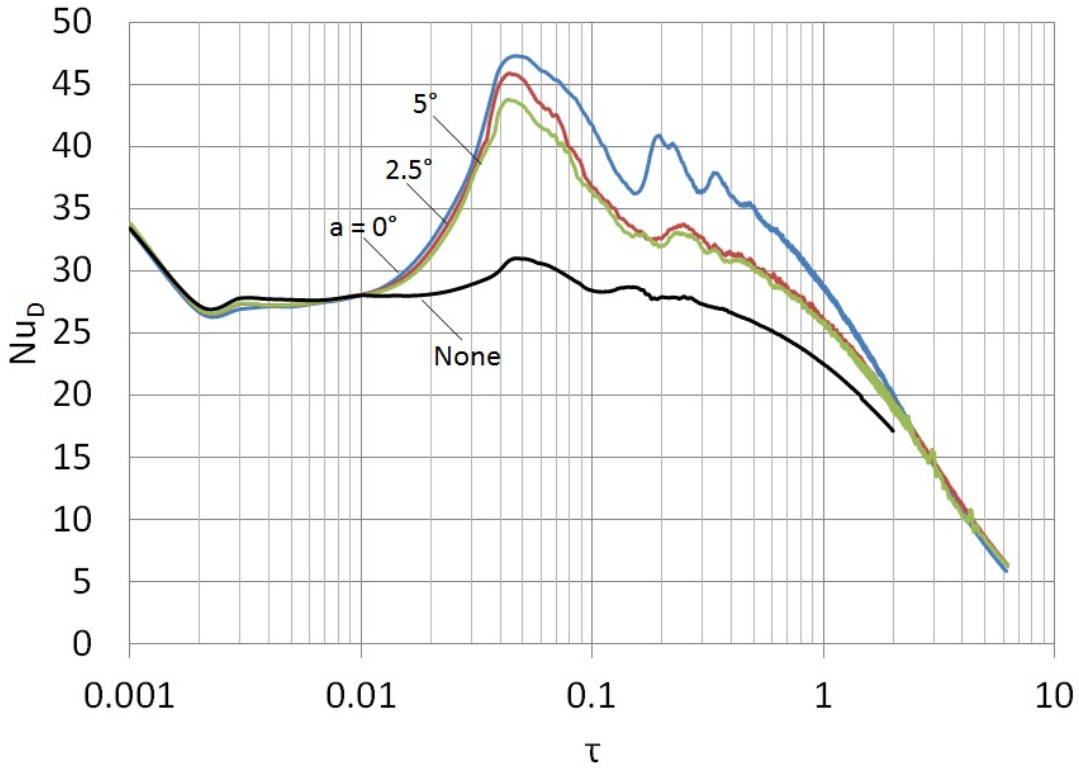

Figure 3.17. Average Nusselt number versus dimensionless time for $Ra_D = 10^7$, W/D = 0.75 and various shroud angles.

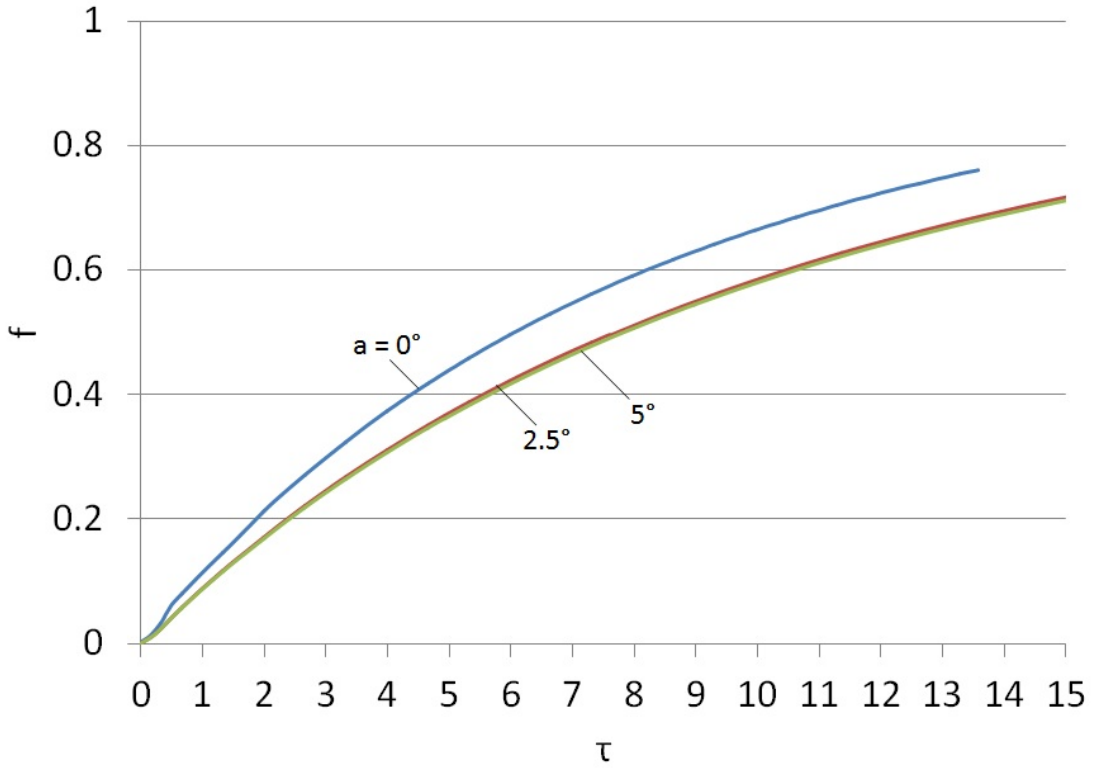

Figure 3.18. Fractional energy discharge versus dimensionless time for $Ra_D = 10^5$, W/D = 0.75 and various shroud angles.

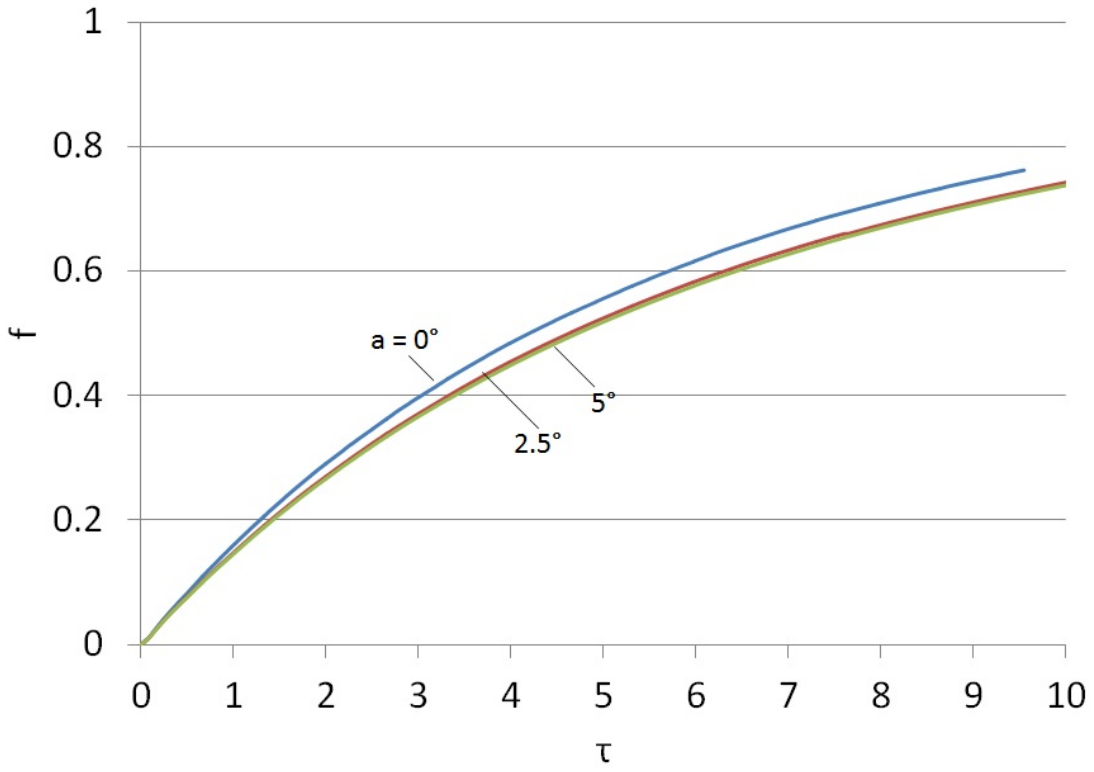

Figure 3.19. Fractional energy discharge versus dimensionless time for $Ra_D = 10^6$, W/D = 0.75 and various shroud angles.

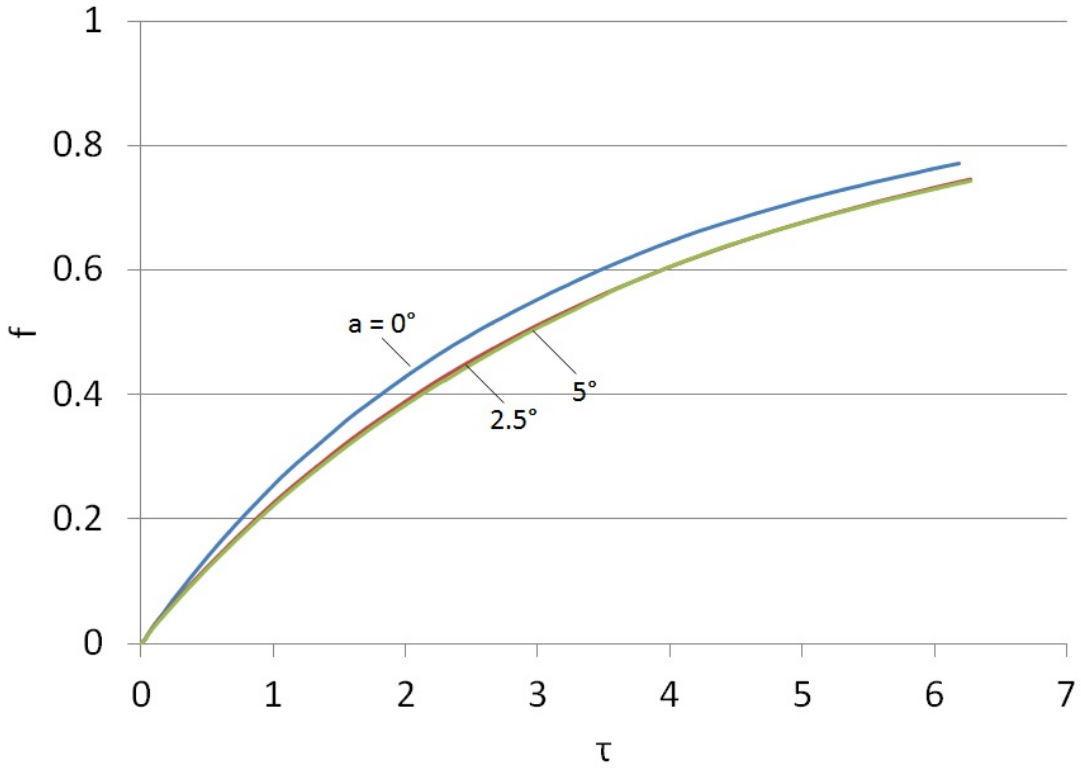

Figure 3.20. Fractional energy discharge versus dimensionless time for $Ra_D = 10^7$, W/D = 0.75 and various shroud angles.

Chapter IV

Conclusion

The present study investigates the width of a shroud and baffle on the heat transfer rate from an immersed heat exchanger in the discharge mode of a solar thermal store. The heat exchanger is modeled as a two-dimensional isothermal cylinder that is situated in a solar thermal storage tank with adiabatic walls. The baffle length and the shroud height and geometry were held constant as the width (or distance away from the heat exchanger) was parametrically varied. An optimal width increases the velocity near the vicinity of the heat exchanger. Numerical simulations were performed for $10^5 < Ra_D < 10^7$ and Pr = 3. Findings suggest that a baffle width 75% less than the width of the heat exchanger is optimal in improving heat transfer performance.

In studying the effects of varying the shroud tilt angle to improve the heat transfer rate, it was determined that varying the angle negatively affected the heat transfer rate. It was proposed that increasing the angle of the opening would increase the heat transfer rate for the designs that choked the flow. In varying the shroud tilt angle, the heat transfer rate decreased compared to the optimum baffle configuration of 75% less than the width of the heat exchanger.

Future Work

The effects of varying the width between the baffle and heat exchanger and the shroud tilt angle to passively improve the heat transfer rate were investigated. These were two parameters that were varied to increase the heat transfer rate, but additional parameters like shroud shape, immersed heat exchanger design, and baffle angle can be investigated. Varying these additional parameters, like changing the shroud shape to an

elliptical or hexagonal shape, increasing the surface area of the immersed heat exchanger, and varying the baffle angle, could increase the heat transfer rate in the solar thermal store.

It was determined that the shroud and baffle created a vena contracta near the surface of the immersed heat exchanger, which caused the speed of the flow to increase locally. To verify the vena contracta, an experiment using a particle image velocimetry system (PIV) can be designed to analyze the velocity field along the near wall of the immersed heat exchanger.

This study was used to determine which parameters will increase the heat transfer rate in a solar thermal storage tank. To verify the results from the numerical simulations, a solar thermal storage tank will be constructed so real life experiments can be conducted. Experiments will be conducted to determine which parameters have the greatest effect on the heat transfer rate in the solar thermal storage tank.

References

[1] Wade, A., Davidson, J., and Haltiwanger, J., 2009. "What is the best solution to improve thermal performance of storage tanks with immersed heat exchangers-baffles or a partitioned tank?" *Journal of Solar Energy Engineering*, **131**, p. 034503.

[2] Mote, R., Probert, S. D., and Nevrala, D., 1991a. "The performance of a coiled finned-tube heat exchanger submerged in a hot-water store: The effect of the exchanger's orientation." *Applied Energy*, **38**, pp. 1-19.

[3] Mote, R., Probert, S. D., and Nevrala, D., 1991b. "Free-convective flows within a hot-water store, induced by a submerged, relatively cold heat exchanger." *Applied Energy*, **39**, pp. 207-234.

[4] Mote, R., Probert, S. D., and Nevrala, D., 1992. "Rate of heat recovery from a hot-water store: Influence of the aspect ratio of a vertical-axis open-ended cylinder beneath a submerged heat-exchanger." *Applied Energy*, **41**, pp. 115-136.

[5] Chauvet, L. P., Nevrala, D. J., and Probert, S. D., 1993b. "Influences of baffles on the rate of heat recovery via a finned-tube heat-exchanger immersed in a hot-water store". *Applied Energy*, **45**, pp. 191-217.

[6] Su, Y., and Davidson, J., 2008. "Discharge of thermal storage tanks via immersed baffled heat exchangers: Numerical model of flow and temperature fields." *Journal of Solar Energy Engineering*, **130**, pp. 021016-1-021016-7.

[7] Haltiwanger, J., and Davidson, J., 2009. "Discharge of thermal storage tank using an immersed heat exchanger with an annular baffle." *Solar Energy*, **83**, pp. 193-201.

[8] Kulacki, F. A., Davidson, J. H., and Herbert, M., 2007. "On the effectiveness of baffles in indirect solar storage systems." *Journal of Solar Energy Engineering*, **129**, pp. 494-498.

[9] Boetcher, S., Kulacki, F., and Davidson, J., 2010. "Negatively buoyant plume flow in a baffled heat exchanger." *Journal of Solar Energy Engineering*, **132**, pp. 034502-1 034502-7.

[10] Boetcher, S., Kulacki, F., and Davidson, J., 2012. "Use of a shroud and baffle to improve natural convection to immersed heat exchangers." *Journal of Solar Energy Engineering*, **134**, pp. 011010-1 011010-7.

[11] Su, Y., and Davidson, J. H., 2005. "Natural convection heat transfer in a collector storage with an immersed heat exchanger: Numerical study." *Journal of Solar Energy Engineering*, **127**, pp.324-332.

[12] Morgan, V. T., 1975. "The overall convective heat transfer from smooth circular cylinders." *Adv. Heat Transfer*, **11**, pp. 199-264.

[13] Churchill, S., and Chu, H., 1975. "Correlating equations for laminar and turbulent free convection from a horizontal cylinder." *International Journal of Heat and Mass Transfer*, **18**, pp. 1049-1053.

[14] Reindl, D. T., Beckman, W. A., and Mitchell, J. W., 1992b. "Transient natural convection in enclosures with application to solar thermal storage tanks." *Journal of Solar Energy Engineering*, **114**, pp. 175-181.